Monthly Notices
of the
ROYAL ASTRONOMICAL SOCIETY

Mon. Not. R. Astron. Soc. **420,** 283–290 (2012) doi:10.1111/j.1365-2966.2011.20031.x

Pulsation models for the roAp star HD 134214

H. Saio,[1⋆] M. Gruberbauer,[2⋆] W. W. Weiss,[3⋆] J. M. Matthews[4⋆] and T. Ryabchikova[5⋆]

[1]*Astronomical Institute, Graduate School of Science, Tohoku University, Sendai 980-8578, Japan*
[2]*Department of Astronomy and Physics, Saint Mary's University, Halifax, NS B3H 3C3, Canada*
[3]*Institute for Astronomy, University of Vienna, Türkenschanzstrasse 17, A-1180 Vienna, Austria*
[4]*Department of Physics and Astronomy, University of British Columbia, 6224 Agricultural Road, Vancouver, BC V6T 1Z1, Canada*
[5]*Institute of Astronomy, Russian Academy of Sciences, Pyatnitskaya 48, 119017 Moscow, Russia*

Accepted 2011 October 18. Received 2011 October 15; in original form 2011 September 23

ABSTRACT

Precise time series photometry with the *MOST* satellite has led to identification of 10 pulsation frequencies in the rapidly oscillating Ap (roAp) star HD 134214. We have fitted the observed frequencies with theoretical frequencies of axisymmetric modes in a grid of stellar models with dipole magnetic fields. We find that, among models with a standard composition of $(X, Z) = (0.70, 0.02)$ and with suppressed convection, eigenfrequencies of a $1.65\,M_\odot$ model with $\log T_{\rm eff} = 3.858$ and a polar magnetic field strength of 4.1 kG agree best with the observed frequencies. We identify the observed pulsation frequency with the largest amplitude as a deformed dipole ($\ell = 1$) mode, and the four next largest amplitude frequencies as deformed $\ell = 2$ modes. These modes have a radial quasi-node in the outermost atmospheric layers ($\tau \sim 10^{-3}$). Although the model frequencies agree roughly with observed ones, they are all above the acoustic cut-off frequency for the model atmosphere and hence are predicted to be damped. The excitation mechanism for the pulsations of HD 134214 is not clear, but further investigation of these modes may be a probe of the atmospheric structure in this magnetic chemically peculiar star.

Key words: stars: chemically peculiar – stars: individual: HD 134214 – stars: magnetic field – stars: oscillations.

1 INTRODUCTION

HD 134214 (HI Lib) is a cool Ap (CP2) star with a spectral type of F2 Sr Eu Cr (Renson & Manfroid 2009). Kreidl (1985) and Kreidl & Kurtz (1986) discovered light variations in this star with a period of 5.65 min, confirming HD 134214 as a member of class of rapidly oscillating Ap (roAp) stars. The roAp class, established by Kurtz (1982), now consists of about 40 known members (see, for a list of members, Kurtz et al. 2006a). The 5.65-min period of HD 134214 is the shortest known among the roAp stars. Only one frequency was detected in the first observations, in later ground-based photometry (Kreidl et al. 1994) and in 10 h of photometric monitoring by the *MOST* satellite in 2006 (Cameron et al. 2006).

The monoperiodicity of HD 134214 was rejected after 2 h of time-resolved spectroscopy by Kurtz, Elkin & Mathys (2006b) who detected five additional frequencies in the radial velocities of some lines of rare-earth elements. Soon after, 8.8 h of spectroscopy by Kurtz et al. (2007) led to the identification of two more frequencies. Furthermore, new photometry they obtained revealed a second significant frequency in light. Kurtz et al. (2007) found that the photometric amplitude ratio of the secondary to the principal frequencies (≈0.17) is similar to the ratio in radial velocity amplitudes. Recently, Gruberbauer et al. (2011) detected 10 independent oscillation frequencies in HD 134214 from a 26-d (2008 April–May) photometric time series obtained by *MOST*, confirming all eight previously reported frequencies. HD 134214 is now one of the richest multiperiodic roAp stars known, comparable to HD 24712 (HR 1217) (Kurtz et al. 2005), HD 101065 (Przybylski's star) (Mkrtichian et al. 2008) and HD 60435 (Matthews, Kurtz & Wehlau 1987).

The pulsations observed in roAp stars are p modes of low degree and high radial order, affected by globally coherent magnetic fields of strengths $1 \leq B \leq 25$ kG. The periods range from 5.6 to 21 min. The amplitudes of many roAp pulsation modes are modulated with the star's rotation period. This has been explained by the oblique pulsator model proposed by Kurtz (1982), in which the pulsation is axisymmetric with respect to the dipole magnetic axis, which is itself obliquely inclined to the stellar rotation axis by an angle β. However, no amplitude modulation has been observed in HD 134214 in any of the photometric or spectroscopic data obtained to date. This may indicate that the magnetic obliquity is small

⋆E-mail: saio@astr.tohoku.ac.jp (HS); mgruberbauer@ap.smu.ca (MG); werner.weiss@univie.ac.at (WWW); matthews@astro.ubc.ca (JMM); ryabchik@inasan.ru (TR)

($\beta \approx 0^\circ$), or that the rotation axis is nearly coincident with the line of sight ($i \approx 0^\circ$) (Kreidl & Kurtz 1986).

How does the strong magnetic field of an roAp star affect its pulsations? Lorentz forces on the moving plasma in the stellar atmosphere mean that the angular dependence of the eigenfunction of a non-radial mode cannot be described by a single spherical harmonic. In addition, p-mode (acoustic) oscillations couple with magnetic oscillations in the outer layers where the Alfvén velocity (v_A) is comparable to the sound speed (c_s). Due to this coupling, part of the acoustic oscillation energy is converted to magnetic oscillations which propagate inwards as slow waves. These slow waves are expected to be dissipated deep in the interior of the star because of their very short spatial wavelengths (Roberts & Soward 1983); i.e. magnetic coupling damps the p-mode oscillations. Including these effects, the properties of adiabatic p-mode oscillations in the presence of dipole magnetic fields were first investigated by Dziembowski & Goode (1996), Bigot et al. (2000), Cunha & Gough (2000) and Saio & Gautschy (2004). The results from different methods qualitatively agree with each other (Saio 2008). The oscillation frequency of a p mode generally increases as the strength of the magnetic field increases, because the phase velocity of magneto-acoustic waves $\sqrt{c_s^2 + v_A^2}$ increases. The gradual frequency increase is interrupted occasionally by an abrupt fall of a few tens of μHz, when the damping due to slow-wave dissipation reaches a peak (Cunha & Gough 2000; Saio & Gautschy 2004).

Cunha (2006) modified the method of Cunha & Gough (2000) to make it possible to treat quadrupole magnetic fields, while Saio (2005) extended the method of Saio & Gautschy (2004) to non-adiabatic oscillations. Furthermore, Bigot & Dziembowski (2002) and Bigot & Kurtz (2011) found that pulsation axis does not necessary align with the magnetic axis if rotational effects are taken into account. Theoretical pulsation analyses including magnetic effects have been applied to several roAp stars to fit observed frequencies; for example, γ Equ (Gruberbauer et al. 2008), 10 Aql (Huber et al. 2008), HD 101065 (Mkrtichian et al. 2008), HD 24712 (=HR 1217; Saio, Ryabchikova & Sachkov 2010) and three roAp stars recently found by the *Kepler* satellite (Balona et al. 2011a,b; Kurtz et al. 2011).

In this paper, we compare oscillation frequencies of HD 134214 obtained by Gruberbauer et al. (2011) from 2008 *MOST* photometry to theoretical frequencies of axisymmetric low-degree modes calculated by the method of Saio (2005), including the effect of dipole magnetic fields.

2 FUNDAMENTAL PARAMETERS OF HD 134214

In the literature, we note two recent sets of estimates of luminosity and effective temperature: $\log L/L_\odot = 0.882 \pm 0.083$ and $\log T_{\rm eff} = 3.849 \pm 0.018$ by Hubrig, North & Mathys (2000), and $\log L/L_\odot = 0.85 \pm 0.07$ and $\log T_{\rm eff} = 3.858 \pm 0.012$ by Kochukhov & Bagnulo (2006). In both cases, the *Hipparcos* parallax was used to derive luminosity, and photometric indices of the Strömgren and the Geneva system to obtain $T_{\rm eff}$. Also, Ryabchikova, Kochukhov & Bagnulo (2008) obtained $T_{\rm eff} = 7315$ ($\log T_{\rm eff} = 3.864$) and $\log g = 4.45$ from Strömgren photometry.

The possible locations of HD 134214 in the HR diagram (HRD) set by these estimates are shown in Fig. 1; filled and open circles with error bars are for the Kochukhov & Bagnulo (2006) and Hubrig et al. (2000) estimates, respectively, and the range of $T_{\rm eff}$ obtained by Ryabchikova et al. (2008) is shown near the bottom of the diagram. Also shown in this figure are the positions of other roAp stars (crosses) adopted mainly from Balmforth et al. (2001) and Kochukhov & Bagnulo (2006). This figure indicates that HD 134214 is a relatively cool roAp star and its location in the HRD is similar to that of the prototypical roAp star HD 24712 (=HR 1217). Not only their positions in the HRD are similar, but also their pulsational properties (Gruberbauer et al. 2011). We will return to this similarity later in the paper.

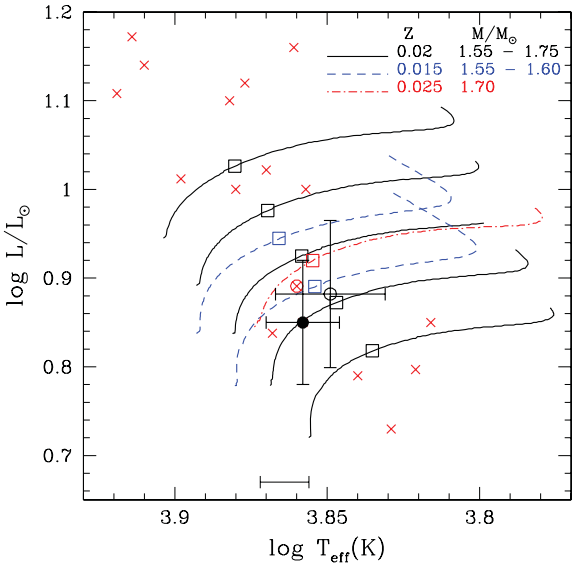

Figure 1. HRD showing evolutionary tracks and the positions of HD 134214 estimated by Kochukhov & Bagnulo (2006) and Hubrig et al. (2000), filled and open circles (with error bars), respectively. The range of $T_{\rm eff}$ near the bottom of the diagram is from Ryabchikova et al. (2008). Crosses show positions of other roAp stars; the circled cross represents HD 24712 (HR 1217). The open square on each evolutionary track indicates the model whose oscillation frequencies best fit the observed frequencies of HD 134214.

Mathys et al. (1997) obtained a mean surface magnetic field $\langle B_s \rangle$ of 3.1 kG from the Zeeman splitting pattern, but found no measurable longitudinal fields in HD 134214. They also found a slight modulation of the mean field strength with a period of 4.15 d, although Adelman (2000) found no long-term variation in the mean light. If the periodicity indicates the rotation period of HD 134214, it corresponds to an equatorial velocity of $\sim$20 km s^{-1}. Combined with the projected rotation velocity $v_e \sin i = 2$ km s^{-1} obtained by Ryabchikova et al. (2008), we find the inclination angle to be as small as $\sim 6^\circ$. Such a nearly pole-on condition in HD 134214 was also inferred from the absence of pulsation amplitude modulations (and no rotational frequency splittings) by Kreidl et al. (1994).

3 STELLAR AND PULSATION MODELS

We have generated unperturbed stellar models for our pulsation analysis from evolution models calculated by a Henyey-type code for a mass range of $1.55 \leq M/M_\odot \leq 1.75$, using OPAL opacity tables (Iglesias & Rogers 1996) supplemented with low-temperature tables by Alexander & Ferguson (1994). Some of the calculated evolutionary tracks are shown in Fig. 1.

For the outermost atmospheric layers, we have employed the standard T–τ relation given in Shibahashi & Saio (1985). In some models, helium is assumed to be depleted above the first He ionization zone (appropriate for the stratified atmosphere of an Ap star) in the same way as described by Saio et al. (2010). We have suppressed envelope convection in majority of the models, assuming

Table 1. Unperturbed model parameters.

Model name	$M/M_\odot$	X	Z	Helium depletion	Envelope convection
D155	1.55	0.700	0.020	Y	N
D160	1.60	0.700	0.020	Y	N
D165	1.65	0.700	0.020	Y	N
D170	1.70	0.700	0.020	Y	N
D175	1.75	0.700	0.020	Y	N
H170	1.70	0.700	0.020	N	N
H160C	1.60	0.700	0.020	N	Y
H165C	1.65	0.700	0.020	N	Y
H170C	1.70	0.700	0.020	N	Y
D155Z15	1.55	0.705	0.015	Y	N
D160Z15	1.60	0.705	0.015	Y	N
D170Z25	1.70	0.695	0.025	Y	N

that a strong magnetic field should inhibit convective instability in the envelope. For those models where we did not suppress envelope convection, we used the mixing-length theory formulated by Henyey, Vardya & Bodenheimer (1965) with a mixing length of 1.5 pressure scaleheights. Core convection is always included, but with no overshooting. Table 1 lists the assumed parameters adopted for each series of evolutionary models, in which 'Y' and 'N' mean 'included' and 'not included', respectively.

We have calculated non-adiabatic frequencies for axisymmetric p modes in the presence of dipole magnetic fields (but without rotation) using the method described by Saio (2005) and Saio & Gautschy (2004), where perturbations of magnetic fields are included by adopting the ideal magnetohydrodynamic approximation. The pulsation axis is assumed to be aligned with the magnetic axis. Frequencies are obtained for field strengths at intervals of 0.1 kG in the range $2\,\mathrm{kG} \le B_\mathrm{p} \le 7\,\mathrm{kG}$ (where B_p = polar field strength). Since the angular dependence of the eigenfunction of a pulsation mode in the presence of a magnetic field deviates from a single spherical harmonic, we express it by a sum of terms proportional to Legendre functions $P_\ell(\cos\theta)$ (or $Y_\ell^{m=0}$, where θ is co-latitude measured from the pulsation axis) with $\ell = 0, 2, 4, \ldots$ for an even mode, or $\ell = 1, 3, 5, \ldots$ for an odd mode, i.e. the kinetic energy of a pulsation mode is distributed among components with different degrees ℓ. To designate the angular dependence of a mode we use ℓ_m which is equal to the degree ℓ of the component having the largest fraction of kinetic energy among the expanded terms of the mode. In most cases, we have employed 12 ℓ values to express an eigenfunction. When the expansion did not converge sufficiently after 12 terms, up to 14 Legendre functions were used.

It is not easy to estimate a mean error for theoretical frequencies, because uncertainty depends on the frequency and B_p. When the convergence of expansion is reasonably good (i.e. the ratio of the kinetic energy of the last component to that of the main component is less than 10 per cent), the differences between the frequencies obtained using 12 and 14 Legendre functions are less than 0.5 μHz. But among the cases with a mediocre convergence with the above ratio being 10–30 per cent, the differences in some cases are ∼1 μHz (in rare cases the difference can be up to 1.5 μHz). From these properties, we consider the mean error of the theoretical frequencies due to the truncation of the expansion to be ∼0.5 μHz. In addition, we expect errors from using spherically symmetric equilibrium models despite strong magnetic fields. Although it is not clear how seriously the magnetic non-sphericity would affect the frequencies of high-order p modes, we assume that the uncertainty in theoretical frequencies would be ∼1 μHz.

Since the observed pulsation frequencies of HD 134214 are all above the acoustic cut-off frequency (as in the case of HD 24712), we have applied the running wave outer boundary condition described in Saio et al. (2010). In the pulsation analysis for models that include envelope convection, we have used a frozen convection approximation for the divergence of convective energy flux. The perturbation of radiative flux is treated in the same way as done by Saio et al. (2010), adopting the Unno & Spiegel (1966) theory for the time-dependent Eddington approximation.

4 FREQUENCY FITTINGS

Table 2 lists frequencies and photometric amplitudes obtained by Gruberbauer et al. (2011) from *MOST* photometry, and radial velocity amplitudes of Nd III lines obtained by Kurtz et al. (2007). The first column contains the designations of frequencies by Gruberbauer et al. (2011), and the second column lists the corresponding designations by Kurtz et al. (2007). No frequencies corresponding to ν_9 and ν_{10} were found by Kurtz et al. (2007). The ranking of the photometric amplitudes is very different from that of the radial velocity amplitudes (except for ν_1) which might be related to differences in mode properties and/or long-time variations in pulsation amplitudes (Kurtz et al. 2007). The last column of the table indicates ℓ_m for each frequency identified in our best models (see below).

For the fittings to be discussed in this section, we adopt only the eight confirmed frequencies ($\nu_1, \nu_2, \ldots, \nu_8$) common to both the photometric and spectroscopic analyses. We omit the two frequencies having lowest amplitudes (ν_9 and ν_{10}), allowing for the possibility that they could be modes of higher degree ($\ell_\mathrm{m} \ge 4$). We will discuss later the result of fits including all 10 frequencies.

For each model sequence listed in Table 1, we have looked for a model whose frequencies of low-degree ($\ell_\mathrm{m} \le 3$) axisymmetric modes best fit the eight frequencies ($\nu_1, \nu_2, \ldots, \nu_8$). The 'goodness' of a model fit is measured by the mean deviation (MD) from the eight frequencies, where we have adopted the same weight for all eight, because the uncertainties in observed frequency values (0.05 μHz) are much smaller than theoretical ones (∼1 μHz). The theoretical frequencies have been interpolated with respect to radius along each evolutionary path to find the best radius, but no interpolation is performed with respect to B_p because frequency may change discontinuously as a function of B_p. (Recall that model frequencies are calculated at intervals of 0.1 kG.)

Table 3 lists parameters of the best fitting models we have found for various model sequences; the MDs are given in the last

Table 2. Observed frequencies and amplitudes of HD 134214.

ID1[a]	ID2[b]	Freq.[a] (mHz)	Amp.[a] (mmag)	Amp.(Nd III)[b] ($\mathrm{m\,s^{-1}}$)	ℓ_m
ν_1	ν_{k1}	2.9495	1.820	374.3	1
ν_2	ν_{k6}	2.9157	0.174	22.1	2
ν_3	ν_{k2}	2.7795	0.157	60.6	2
ν_4	ν_{k7}	2.9833	0.116	22.4	2
ν_5	ν_{k3}	2.6470	0.063	36.4	2
ν_6	ν_{k5}	2.7220	0.061	38.8	1
ν_7	ν_{k8}	2.8053	0.054	19.4	0
ν_8	ν_{k4}	2.8416	0.051	22.5	3
ν_9	–	2.6872	0.048	–	1?
ν_{10}	–	2.6998	0.044	–	3?

[a]Adopted from Gruberbauer et al. (2011).
[b]Adopted from Kurtz et al. (2007).

Table 3. Best-fitting models.

Model	$\log R$	$\log T_{\rm eff}$	$\log L$	$B_{\rm p}$(kG)	MD(μHz)
D155	0.2623	3.8352	0.8180	4.8	1.31
D160	0.2659	3.8470	0.8723	4.4	1.29
D165	0.2694	3.8584	0.9250	4.1	1.23
D170	0.2728	3.8695	0.9761	3.8	1.33
D175	0.2761	3.8803	1.0262	3.9	1.29
H170	0.2740	3.8691	0.9769	4.3	1.32
H160C	0.2707	3.8453	0.8753	7.0	1.22
H165C	0.2729	3.8572	0.9271	5.9	1.20
H170C	0.2747	3.8689	0.9773	4.6	1.28
D160Z15	0.2645	3.8658	0.9448	4.3	1.32
D170Z25	0.2740	3.8548	0.9197	4.3	1.26

column. The loci of these best-fitting models in the HRD are shown by open squares in Fig. 1. The MDs of the best models for different masses vary only slightly. A model with $1.65\,{\rm M}_\odot$ best reproduces the eight observed frequencies at polar magnetic field strength $B_{\rm p} = 4.1$ kG among the D sequences, in which a standard composition $(X, Z) = (0.70, 0.02)$ is adopted, envelope convection is suppressed, and helium above the first He ionization zone is depleted. The required magnetic field strength is plausible, given the mean modulus (3.1 kG) for this star obtained spectroscopically (Mathys et al. 1997). Fig. 2 compares the theoretical frequencies of the best model as a function of $B_{\rm p}$ with the observed frequencies; the closest agreement occurs for $B_{\rm p} = 4.1$ kG (vertical dashed line). Generally, pulsation frequencies increase as the magnetic field

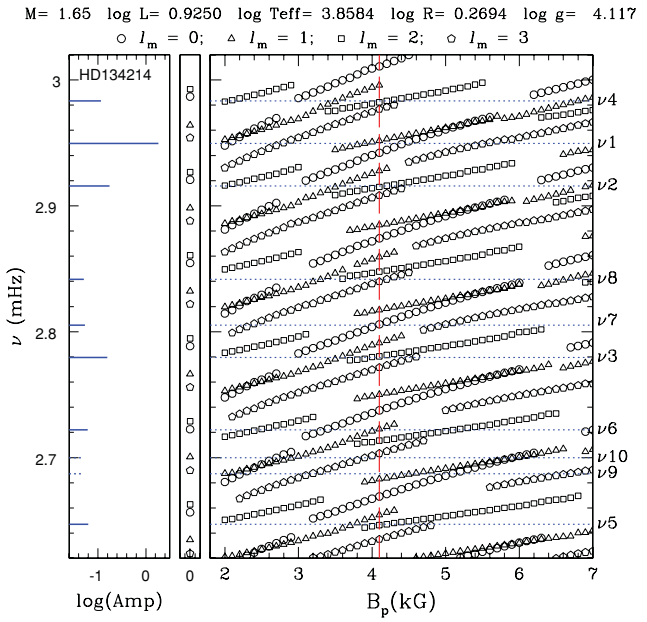

Figure 2. Left-hand panel: observed pulsation frequencies (mHz) and amplitudes (mmag) of HD 134214 obtained by Gruberbauer et al. (2011) from the 2008 *MOST* photometry. Note that the amplitudes are plotted as log values to accommodate the amplitude of the principal frequency (2.950 mHz), which is an order of magnitude larger than any other. Right-hand panel: pulsation frequencies of low-degree modes ($\ell_{\rm m} \le 3$) as a function of polar magnetic strength $B_{\rm p}$ for the best-fitting model of mass $1.65\,{\rm M}_\odot$, whose parameters are shown at the top of the diagram. Horizontal dotted lines indicate observed frequencies, whose designations are given along the right vertical axis. The model well reproduces the observed frequencies ν_1, $\nu_2, \ldots, \nu_8$ at $B_{\rm p} = 4.1$ kG (vertical dashed line). Middle (narrow) panel: model frequencies with no magnetic field ($B_{\rm p} = 0$).

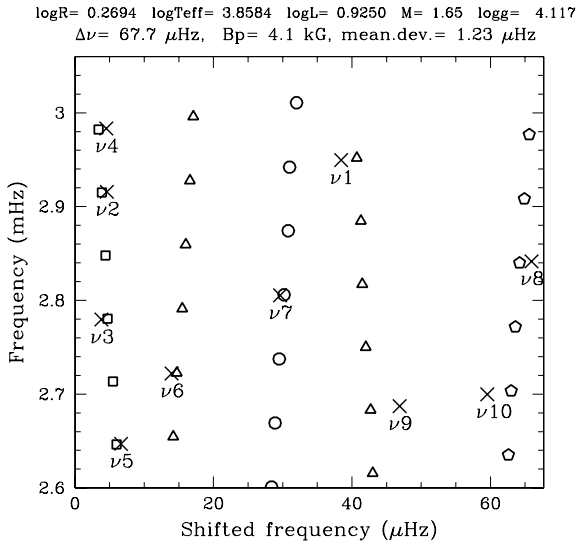

Figure 3. Echelle diagram (folded modulo 67.7 μHz) for the best-fitting model with polar magnetic field strength $B_{\rm p} = 4.1$ kG of the D165 ($1.65\,{\rm M}_\odot$) model sequence. Crosses are observed frequencies whose designations are taken from Gruberbauer et al. (2011). Open circles, triangles, squares and pentagons represent theoretical frequencies for $\ell_{\rm m} = 0$, 1, 2 and 3, respectively. MD is shown for $\nu_1, \nu_2, \ldots, \nu_8$.

strength increases, roughly preserving the large separation. However, since the dependence of frequencies on $B_{\rm p}$ differs slightly for different $\ell_{\rm m}$, the relative loci of sequences for different degrees $\ell_{\rm m}$ differ considerably from the case with no magnetic field.

The slow increase in frequency with $B_{\rm p}$ is interrupted occasionally by a sudden decrease of a few tens of μHz; this behaviour was first recognized by Cunha & Gough (2000). Fig. 2 shows that, in such a transition range, two distorted dipole modes appear. This is why two dipole modes appear within a large frequency separation in the echelle diagram shown in Fig. 3. These two deformed dipole modes have $\ell_{\rm m} = 1$ by definition, but have different distributions of kinetic energy among components of $\ell = 3, 5 \ldots$, and hence have different angular dependences. Such additional modes are needed to explain the frequency spectrum of the roAp star HD 101065 (Mkrtichian et al. 2008).

The theoretical frequencies of the model with $B_{\rm p} = 4.1$ kG are compared in detail as an echelle diagram in Fig. 3. In this diagram, frequencies are folded modulo 67.7 μHz according to the large frequency separation obtained by Gruberbauer et al. (2011) from their observed frequencies of HD 134214. The large separation of the model is consistent with the observed one, although the former slightly depends on degree $\ell_{\rm m}$ due to the fact that the magnetic effects also depend on $\ell_{\rm m}$. We find reasonably good agreement between theoretical and observed frequencies. The MD of this model (1.23 μHz) seems to be slightly larger than the uncertainty expected for theoretical frequencies. A non-dipole component of the magnetic field could account for the discrepancy.

We identify the principal frequency ($\nu_1 = 2.950$ mHz) as a distorted dipole mode, while frequencies ν_2, ν_3, ν_4 and ν_5 are identified as $\ell_{\rm m} = 2$ modes. We note that the frequencies ν_2, ν_3 and ν_4, have similar amplitudes (next largest after the principal frequency) and, hence, appear to share the same degree. Mode identifications in the other best-fitting models listed in Table 3 are similar to those by D165. They are listed in the last column of Table 2.

Comparing the best models of the D170 and H170 sequences, we see that helium depletion in the upper atmosphere does not affect the

'goodness' of the best model. The magnetic field strength of the best fit from the helium-depleted model sequence (D170) is smaller than the model without helium depletion (H170). A stronger magnetic field is needed for the latter model to have the same magnetic effect, because the mean density of the model without helium depletion is larger than the helium-depleted model at the same L and $T_{\rm eff}$, due to the lower opacity and higher mean-molecular weight.

It can be seen in Table 3 that including convective energy transport in the envelope convection zone (H160C, H165C and H170C) slightly improves the quality of the fits but only by adopting stronger magnetic fields. The improvement, however, seems too weak to claim the presence of efficient convection in the polar regions of HD 134214. The necessity of the stronger fields is due to higher mean density in the outer envelope as discussed above. In this case, the higher density is caused by, in addition to the homogeneous helium abundance in the envelope, a decrease in the temperature gradient brought by convective energy transport. Changing metallicity does not significantly change the quality of fits.

5 MODE PROPERTIES

In the best-fitting models discussed above, the principal frequency corresponds to a deformed dipole mode, while $\nu_2 \cdots \nu_5$ match $\ell_{\rm m} = 2$ modes whose amplitudes are very much smaller than that of the principal one (see Table 2). One could speculate that the large amplitude difference might be a difference in visibility due to different angular dependences of the amplitudes on the stellar surface between modes of $\ell_{\rm m} = 1$ and 2. However, a glance at Fig. 4 demonstrates that this is not the case. This figure shows the latitudinal dependences of flux perturbations of the dipole mode (solid line) and one of the $\ell_{\rm m} = 2$ modes, ν_3 (short dashed line) for $B_{\rm p} = 4.1$ kG. The latitudinal dependences are similar to each other, although without a magnetic field, a dipole mode should vary as $\cos\theta$, quite different from the expected $\ell = 2$ dependence $[(1/2)(3\cos^2\theta - 1)]$. The strong magnetic field suppresses pulsation amplitudes at low latitudes because gas cannot cross field lines, so that large amplitudes are strongly confined to the polar regions.

The only appreciable difference between the two modes is the parity with respect to the equatorial plane; $\ell_{\rm m} = 1$ modes are odd and $\ell_{\rm m} = 2$ modes are even. For the principal frequency to be identified as a deformed dipole mode, the angle between the magnetic axis and line of sight should be small so that the contribution from the opposite hemisphere is small. Combining this fact with the requirement of a small angle between the rotation axis and the line of sight (Section 2) indicates the obliquity angle β of HD 134214 must be small too. With a small angle between the line of sight and the pulsation axis, there is little difference in the visibility between $\ell_{\rm m} = 1$ and 2 modes. This is contrary to the conjecture of Gruberbauer et al. (2011) that the large amplitude difference between ν_1 and other frequencies is due to a large difference in their visibilities.

Fig. 4 also shows the latitudinal distributions of flux perturbation for $\ell_{\rm m} = 0$ and 3 modes which are fitted to ν_7 and ν_8, respectively. In contrast to the cases of $\ell_{\rm m} = 1$ and 2, the flux amplitudes of the $\ell_{\rm m} = 0$ and 3 modes show wavy variations as a function of latitude with quasi-nodal lines which would reduce the visibility of the modes. (Note that the $\ell_{\rm m} = 0$ mode is significantly deformed from spherical symmetry due to the contributions from high ℓ components.) This is consistent with the fact that ν_7 and ν_8 have smallest amplitudes among the eight frequencies adopted here.

Fig. 5 shows runs of phase delay and amplitude of radial velocity variations in the atmosphere of a model which has parameters close to those of the best (interpolated) model. In this figure, the pulsation

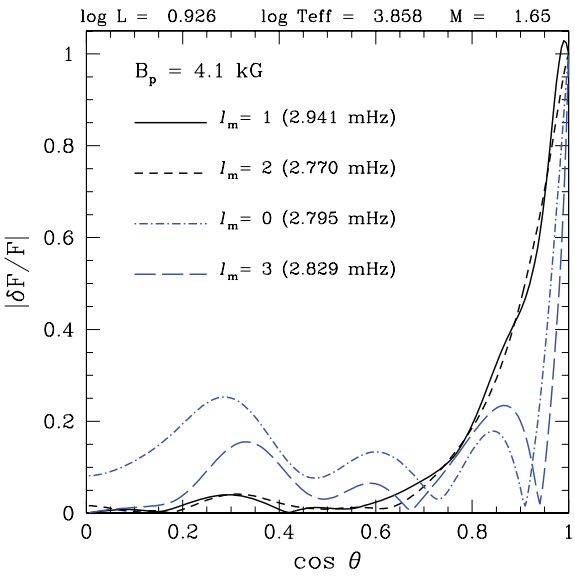

Figure 4. The latitudinal amplitude distribution of flux perturbation as a function of co-latitude θ on the stellar surface of a model with $M = 1.65\,{\rm M}_\odot$ and $B_{\rm p} = 4.1$ kG. The solid line is for a deformed dipole mode which fits the principal frequency of HD 134214, the short dashed line for a $\ell_{\rm m} = 2$ mode fitted to $\nu_3 (= \nu_{\rm k2})$, the dot–dashed line for a $\ell_{\rm m} = 0$ mode fitted to ν_7, and the long dashed line for a $\ell_{\rm m} = 3$ mode fitted to ν_8.

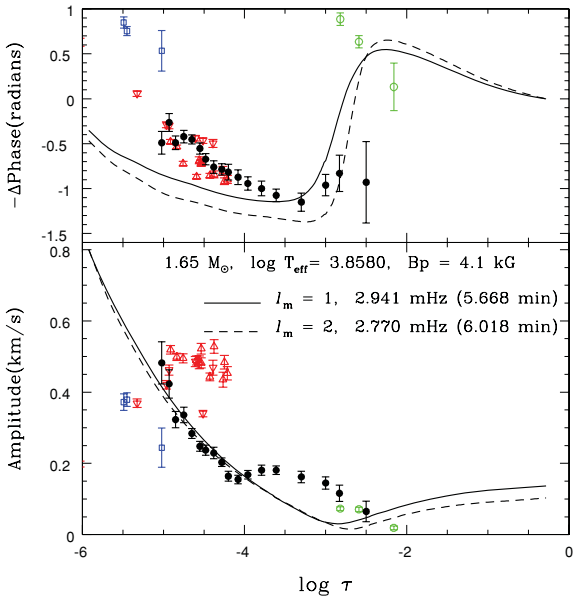

Figure 5. Pulsation phase (top panel) and radial velocity amplitude (bottom panel) variations in the atmosphere of a $1.65\,{\rm M}_\odot$ model close to the best-fitting model with $B_{\rm p} = 4.1$ kG, for ν_1 (solid lines) and $\nu_3 (= \nu_{\rm k2})$ (dashed lines). The radial velocity amplitude is set to be 0.8 km s^{-1} at $\log\tau = -6$, while the phase is set to be zero in the photosphere, where τ is the optical depth calculated with the Rosseland mean opacity. In this diagram, the pulsation (and hence magnetic) axis is assumed to be along the line of sight. Also shown are radial velocity data of HD 134214 taken from Ryabchikova et al. (2007); • = bisector of Hα core, ◯ = Y II, △ = Nd II, ▽ = Nd III and □ = Pr III, where the optical depth at each Hα line depth and the formation depths of the other lines are assumed to be the same as in the case of HD 24712.

axis (and hence the magnetic axis) is assumed to be aligned with the line of sight. The properties are not very sensitive to the obliquity of pulsation and magnetic axes; we see very similar model behaviours if we adopt, for example, an obliquity of 30° instead of 0°. Fig. 5 reveals a quasi-node around $\log \tau \approx -3$ for both modes, where τ is again the optical depth calculated with the Rosseland mean opacity. Above the quasi-node, the amplitude and phase delay increase outwards, indicating the presence of outwardly running wave components. This is consistent with the fact that both frequencies are above the critical acoustic cut-off. We note that the quasi-node is not the 'false node' discussed by Sousa & Cunha (2011), because it appears in the eigenfunction.

Also plotted in Fig. 5 are data of radial velocity/phase measurements from Hα bisector and lines of some rare-earth elements of HD 134214 adopted from Ryabchikova et al. (2007), where the optical depth at each Hα line depth and the formation depths of the other lines are assumed to be the same as in the case of HD 24712. This figure shows that the observational data qualitatively agree with the model; amplitude and phase delay increases outwards in the outermost layers, which also agree with the spectroscopic analysis by Kurtz et al. (2007). However, the observed variation of phase delay in the outermost layers is considerably steeper than the model prediction. The discrepancy probably indicates that the sound speed (or temperature) in the upper atmosphere of HD 134214 is lower than in the model. This is consistent with the actual temperature gradient being steeper due to a strong blanketing effect which is not included in our models.

The radial velocity amplitudes measured by Nd II/Nd III tend to be larger than those of Hα, while the amplitudes of Pr III lines tend to be smaller than those of Hα. These differences can be attributed to the difference in the distributions of the elements Nd and Pr on the stellar surface. If the depths of line formation are similar to HD 24712, as we have surmised, then Figs 4 and 5 suggest that Nd is distributed at a higher pulsational latitude than Pr.

At the quasi-node, the pulsation phase of the principal frequency ν_1 changes dramatically by about 1.8 rad. The presence of the phase shift at $\tau \approx -3$ is supported observationally by the phase shift from the deep part of Hα phase to the phases of Y II (Fig. 5).

The runs of phase and amplitude in the atmosphere for $\nu_3 (=\nu_{k2}$; $\ell_m = 2)$ shown in dashed lines in Fig. 5 are very similar to those for the principal frequency ($\ell_m = 1$; solid lines). This agrees with the finding by Kurtz et al. (2007) that the amplitude ratio of the two frequencies (ν_1 and ν_3) from the radial velocity variations (weighted towards the outermost layers) is similar to that measured for the light variations (which occur in the photosphere).

The similarity in the latitudinal and depth dependences between the principal mode and the secondary mode suggests that the huge amplitude difference is caused by a large difference in the excitation strengths of yet unknown mechanism.

6 FITTING ALL 10 FREQUENCIES

In the model fits described above, we omitted the two frequencies (ν9 and ν10) with the lowest amplitudes because they might be due to high-degree ($\ell_m \geq 4$) modes for which no theoretical frequencies are available. Here we discuss fits performed for models in the D165 sequence assuming all 10 observed frequencies are low-degree ($\ell_m \leq 3$) modes. Fig. 6 shows the echelle diagram for the best-fitting model from the D165 series. The observed frequencies are best fitted with $B_p = 4.2$ kG, resulting in a mean deviation, MD = 2.18 μHz. Compared to the best-fitting D165 model for only eight frequencies (Table 3), this model is slightly hotter, but still within the uncertainty of the photometric effective temperature (Fig. 1). Note that in Fig. 6 frequencies are folded with a separation of 70.6 μHz, which is larger than what is used in Fig. 3 (67.7 μHz) because of the higher $T_{\rm eff}$. In this model, (ν_4, ν_2, ν_8, ν_{10}) are identified as $\ell_m = 2$ modes rather than (ν_4, ν_2, ν_3, ν_5). Comparing Fig. 6 (10-frequency fit) with Fig. 3 (8-frequency fit), the quality of fit is better in the latter case. This is circumstantial evidence supporting the argument that ν_9 and ν_{10} are modes of degree equal to or higher than 4.

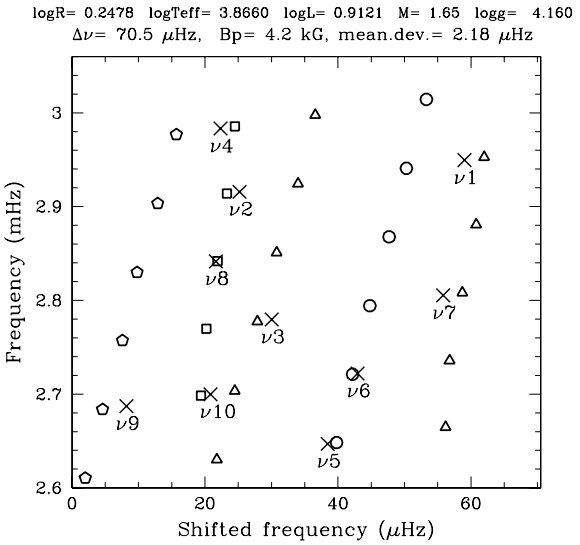

Figure 6. An echelle diagram (folded modulo 70.5 μ Hz) for the model (among models of D165) which best fits (with a MD of 2.18 μ Hz) the 10 observed pulsation frequencies of HD 134214. The model has a polar field strength of $B_p = 4.2$ kG. Symbols are the same as in Fig. 3.

7 DISCUSSION

7.1 Excitation mechanism

The predicted frequencies and large separations of the best-fitting model of each series are roughly consistent with the observed values for HD 134214. However, there is one serious problem: all observed frequencies are above the acoustic cut-off frequencies of our models and all modes with appropriate frequencies are damped modes.

Pulsations of roAp stars are now generally considered to be excited by the κ-mechanism operating in the hydrogen ionization zone (Balmforth et al. 2001; Cunha 2002). Our models are located in the instability region of the HRD obtained by Cunha (2002). It turns out that p-mode pulsations of order up to $n \sim 20$ ($\nu \lesssim 1.4$ mHz) are actually excited by the κ-mechanism in the best-fitting D165 model ($B_p \sim 4$–5 kG). But none of these predicted pulsations has been detected.

Audard et al (1998) found that the cut-off frequency increases if the T–τ relations based on more physically accurate atmospheric models are used. For the $T_{\rm eff}$ range appropriate for HD 134214, however, even their models predict cut-off frequencies below about 2.7 mHz, smaller than the principal frequency of 2.95 mHz in HD 134214. Another way to increase the cut-off frequency is to introduce a temperature inversion in the atmosphere, as proposed by Gautschy, Saio & Harzenmoser (1998). Unfortunately, the inversion necessary in this case must be a few thousand degrees. Even if we assume a reflective boundary condition, no modes having frequencies comparable to those of HD 134214 are excited. In addition,

observations indicate the presence of outwardly running waves in the outermost layers (Fig. 5) do not support a reflective boundary. Therefore, the outer boundary is probably not the cause of the excitation discrepancy.

The same problem exists for another multiperiodic roAp star, HD 24712 (HR 1217), as discussed by Saio et al. (2010). These two examples clearly indicate that an instability mechanism other than the κ-mechanism must be operating, at least for the supercritical frequency pulsations. The mechanism must be intimately connected with the interaction with magnetic fields because no such high-frequency oscillations occur in A–F stars other than the roAp stars. The atmospheric layers with a super-adiabatic temperature gradient and a magnetic field are overstable in linear analyses with the Boussinesque approximation, where density perturbations are neglected except for buoyancy forces (e.g. Chandrasekhar 1961). Based on the fact that the periods of overstability for Ap stars with reasonable magnetic field strengths are comparable to the period range seen in roAp stars, Shibahashi (1983) predicted overstability to be the excitation mechanism for roAp stars. Cox (1984) discussed some physical implications of overstability. Weaknesses of this concept were identified by Balmforth et al. (2001): as the analyses are local, it is not certain whether a global mode is excited, and even if global modes are excited it is not certain whether such a mode has any significant amplitude above the thin convective layer. Further investigations of the roAp excitation mechanism are definitely needed.

7.2 Similarities and dissimilarities to HD 24712

We have already mentioned several times in this paper the similarity of HD 134214 to another roAp star HD 24712 (HR 1217), and Table 4 compares a few properties of these two stars. The loci in the HRD of the best-fitting models for the two stars are nearly identical. The observed frequency ranges are above the acoustic cut-off frequencies of the models in both cases, and they are predicted to be damped. Both stars have similar large frequency separations and near-zero small separations, δ, which is difficult to reproduce with models. Our best model (shown in Fig. 3) gives $\delta \sim 3\,\mu$Hz, which for HD 134214 is much larger than the observed value of 0.02 μHz. The same difficulty is reported for HD 24712 by Saio et al. (2010). Our current investigation of HD 134214 makes it clear that the problems in modelling of HD 24712 are not unique to this star, and may be the same for other roAp stars with similar parameters.

For completeness, we note some dissimilarities between the two stars. HD 24712 exhibits clear rotational amplitude modulation and associated frequency splittings, while HD 134214 shows none. The amplitude of the principal frequency of HD 134214 (identified by us as an $\ell_{\rm m} = 1$ mode) is very much larger than the other ones and has been nearly constant for a long time (Kurtz et al. 2007; Gruberbauer et al. 2011). On the other hand, HD 24712 has three main frequencies with comparable amplitudes; the relative amplitudes vary on a timescale of a few years (Kurtz et al. 2005).

Table 4. Comparing HD 134214 and HD 24712.

	HD 134214	HD 24712	References
Frequency range (mHz)	2.65–2.98	2.55–2.81	1, 2, 3
Large separation (μHz)	67.7	68	1, 2
Small separation δ^a (μHz)	0.02	0.5	1, 2
Rotational splitting (μHz)	–	0.929	2
Parameters of best-fitting models			4, 5
$\log T_{\rm eff}$	3.8584	3.8585	
$\log L/{\rm L}_\odot$	0.9250	0.9247	
$M/{\rm M}_\odot$	1.65	1.65	
$B_{\rm p}$(kG)	4.1	4.9	

$^a\delta \equiv \nu(l_{\rm m} = 1, n) - 0.5[\nu(l_{\rm m} = 2, n-1) + \nu(l_{\rm m} = 2, n)]$. *References*. 1 = Gruberbauer et al. (2011), 2 = Kurtz et al. (2005), 3 = Mkrtichian & Hatzes (2005), 4 = this paper, 5 = Saio et al. (2010).

8 CONCLUSIONS

We have fitted pulsation models, including magnetic perturbation effects and assuming dipole magnetic geometries, to the frequency spectrum of the rich multiperiodic star HD 134214, which pulsates with the shortest periods known among the roAp stars. We have found that a better fitting is obtained when we fit eight frequencies common to the *MOST* photometry (Gruberbauer et al. 2011) and radial velocity data obtained by (Kurtz et al. 2007), rather than fitting the 10 frequencies obtained by *MOST*. This might indicate that the two new frequencies obtained by Gruberbauer et al. (2011) have high surface degrees of $\ell > 3$.

Among the best-fitting models found in our grid for various input physics, we found that a model with a mass of 1.65 $M_\odot$, effective temperature $\log T_{\rm eff} = 3.8584$, luminosity $\log L/{\rm L}_\odot = 0.9250$ and polar magnetic field strength $B_{\rm p} = 4.1$ kG is the best match to the data. The MD of the fit is 1.23 μHz, which is slightly larger than the expected numerical errors for the model frequencies. Non-dipole components in the magnetic field of HD 134214 may be additional error sources.

The effective temperature and luminosity of the best model are consistent with those derived from multicolour photometry and the *Hipparcos* parallax. We note that the parameters are nearly the same as those of the best model for HD 24712 obtained by Saio et al. (2010).

The principal frequency, with a photometric amplitude 10 times larger than that of the other frequencies, is identified as a deformed dipole mode. The five frequencies with the next largest amplitudes are identified as $\ell_{\rm m} = 2$ modes. In our model, the radial velocity variations of these modes have a quasi-node around $\log\tau \approx -3$, where oscillation phase shifts by $\sim$2 rad. The radial velocity amplitude increases rapidly above the node. These properties qualitatively agree with the data from radial velocity measurements of Hα bisector and lines of rare-earth elements.

Although the model frequencies and amplitude distribution in the atmosphere are consistent with observations of HD 134214, the excitation mechanism is still unknown. The κ-mechanism in the hydrogen ionization zone for example appears to be too weak to excite oscillations in the observed frequency range, above the acoustic cut-off frequency.

Finally, we note that Gruberbauer (2011, in preparation) has recently developed a new probabilistic method for finding a best model in reproducing observed frequencies. One of the advantages of the method is its ability of taking into account the possibility of the presence of systematic errors, which we disregarded completely in this paper. Applying such a probabilistic method to various roAp stars including HD 134214 itself might reveal systematic errors in the model frequencies as a function of the frequency and/or magnetic field strength.

ACKNOWLEDGMENTS

We are grateful to Don Kurtz, the referee of this paper, for his helpful comments and suggestions. MG has received financial support

from an NSERC Vanier scholarship. WWW was supported by the Austrian Research Fund (P22691-N16).

REFERENCES

Adelman S. J., 2000, A&AS, 146, 13
Alexander D. R., Ferguson J. W., 1994, ApJ, 437, 879
Audard N., Kupka F., Morel P., Provost J., Weiss W. W., 1998, A&A, 335, 954
Balmforth N. J., Cunha M. S., Dolez N., Gough D. O., Vauclair S., 2001, MNRAS, 323, 362
Balona L. A. et al., 2011a, MNRAS, 410, 517
Balona L. A. et al., 2011b, MNRAS, 413, 2651
Bigot L., Dziembowski W. A., 2002, A&A, 391, 235
Bigot L., Kurtz D. W., 2011, A&A, in press (arXiv:1110.0988)
Bigot L., Provost J., Berthomieu G., Dziembowski W. A., Goode P. R., 2000, A&A, 356, 218
Cameron C. et al., 2006, Commun. Astroseismology, 148, 57
Chandrasekhar S., 1961, Hydrodynamic and Hydromagnetic Stability. Clarendon, Oxford Press
Cox J. P., 1984, ApJ, 280, 220
Cunha M. S., 2002, MNRAS, 333, 47
Cunha M. S., 2006, MNRAS, 365, 153
Cunha M. S., Gough D. O., 2000, MNRAS, 319, 1020
Dziembowski W. A., Goode P. R., 1996, ApJ, 458, 338
Gautschy A., Saio H., Harzenmoser H., 1998, MNRAS, 301, 31
Gruberbauer M. et al., 2008, A&A, 480, 223
Gruberbauer M. et al., 2011, A&A, 530, 135
Henyey L., Vardya M. S., Bodenheimer P., 1965, 142, 841
Huber D. et al., 2008, A&A, 483, 239
Hubrig S., North P., Mathys G., 2000, ApJ, 539, 352
Iglesias C. A., Rogers R. J., 1996, ApJ, 464, 943
Kochukhov O., Bagnulo S., 2006, A&A, 450, 763
Kreidl T. J., 1985, Inf. Bull. Variable Stars, 2739, 1
Kreidl T. J., Kurtz D. W., 1986, MNRAS, 220, 313
Kreidl T. J., Kurtz D. W., Schneider H., vanWyk F., Roberts G., Marang F., Birch P. V., 1994, MNRAS, 270, 115
Kurtz D. W., 1982, MNRAS, 200, 807
Kurtz D. W., Elkin V. G., Cunha M. S., Mathys G., Hubrig S., Wolff B., Savanov I., 2006a, MNRAS, 372, 286
Kurtz D. W., Elkin V. G., Mathys G., 2006b, MNRAS, 370, 1274
Kurtz D. W., Elkin V. G., Mathys G., van Wyk F., 2007, MNRAS, 381, 1301
Kurtz D. W. et al., 2005, MNRAS, 358, 651
Kurtz D. W. et al., 2011, MNRAS, 414, 2550
Mathys G., Hubrig S., Landstreet J. D., Lanz T., Manfroid J., 1997, A&AS, 123, 353
Matthews J. M., Kurtz D. W., Wehlau W. H., 1987, ApJ, 313, 782
Mkrtichian D. E., Hatzes A. P., 2005, A&A, 430, 263
Mkrtichian D. E., Hatzes A. P., Saio H., Shobbrook R. R., 2008, A&A, 490, 1109
Renson P., Manfroid J., 2009, A&A, 498, 961
Roberts P. H., Soward A., 1983, MNRAS, 205, 1171
Ryabchikova T., Sachkov M., Kochukhov O., Lyashko D., 2007, A&A, 473, 907
Ryabchikova T., Kochukhov O., Bagnulo S., 2008, A&A, 480, 811
Saio H., 2005, MNRAS, 360, 1022
Saio H., 2008, J. Phys. Conf. Ser., 118, 012018
Saio H., Gautschy A., 2004, MNRAS, 350, 485
Saio H., Ryabchikova T., Sachkov M., 2010, MNRAS, 403, 1729
Shibahashi H., 1983, ApJ, 275, L5
Shibahashi H., Saio H., 1985, PASJ, 37, 245
Sousa J. C., Cunha M. S., 2011, MNRAS, 414, 2576
Unno W., Spiegel E. A., 1966, PASJ, 18, 85

This paper has been typeset from a TEX/LATEX file prepared by the author.